

Ann Control Based Energy Harvesting In Freedom System Using Sepic Converter for Multiple DC Microgrid Application

Shijo James¹, G.Sinthana²

¹Assistant Professor, CSI College of Engineering, Ketti

²Student M.E (PED), CSI College of Engineering, Ketti

Abstract- This paper presents a micro grid consisting of different distribution generation(DG) units such as PV, Wind, Fuel cell, battery that are connected to the distribution grid. The proposed micro grid consists of a PV array and wind which functions as the Primary generation unit of the micro grid. A proton exchange membrane fuel cell is used to supplement the variability in the power generated by PV and Wind. A lithium-ion battery is also used to store energy from PV, Wind & Fuel cell and its energy is given to the load/grid during peak energy demand. MPPT is used to extract the maximum output voltage from PV and Wind. Here Perturb and Observation algorithm is used, because it is the simplest MPPT algorithm to get effective output. In standard inverter without the PWM technique, the output voltage changes according to the power consumption of the load. The PWM technology corrects the output voltage greater according to the value of the load by changing the width of the switching frequency in the oscillation section. As a result of this, the AC voltage from the inverter changes depending upon the width voltage of the switching pulse. The PWM controller in the inverter will make correction in the pulse width of the switching pulse based on the feedback voltage and the inverter will give a steady output voltage irrespective of the load characteristics. LC filter is used to eliminate harmonics from the inverter. SEPIC converter is used for output current and voltage regulation. ANN controller is used to eliminate error in the output voltage and maintain constant output voltage at the load/grid side.

Index Terms- DC/DC converter, DC microgrid, Fuzzy logic controller, MPPT, Multiple renewable energy sources, PWM inverter, Storage unit.

I. INTRODUCTION

Over the last decade, efficient and reliable communication and control technologies, coupled

with an increase in smarter electrical facilities, such as electric vehicles and smart meters, have resulted in an increasing number of consumers participating in demand response management (DRM). The current research is also focused on achieving a smarter grid through demand-side management (DSM), increasing energy reserves and improving the power quality of the distribution system, such as harmonic compensation for nonlinear loads [3]. These new trends enable higher levels of penetration of renewable generation, such as Wind, Solar power and Fuel cell into the grid [6][14]. The integration of renewable sources can supplement the generation from the distribution grid. However, these renewable sources are intermittent in their generation and might compromise the reliability and stability of the distribution network. As a result, energy-storage devices, such as batteries and ultra-capacitors, are required to compensate for the variability in the renewable sources [8][12]. The incorporation of energy-storage devices is also critical for managing peak demands and variations in the load demand. In this paper, a microgrid consisting of a photovoltaic (PV) array, Wind, a Proton-exchange membrane fuel cell (PEMFC), and a lithium-ion storage battery (SB) is proposed. The PEMFC is used as a backup generator unit to compensate for the power generated by the intermittent nature of the PV array and Wind. The SB is implemented for peak shaving during grid-connected operation, and to supply power for any shortage in generated power during islanded operation and to maintain the stability of the distribution network. An energy-management which optimizes the steady-state and the transient control problems separately. In this way, the computation time is greatly reduced. In what follows, this paper provides a comprehensive solution for the operation

of a microgrid which will simultaneously dispatch real and reactive power during both grid-connected and islanded operations, compensate for harmonics in the load currents, and perform peak shaving and load shedding under different operating conditions.

II. BOOST-ZETA INTEGRATED CONVERTER

It should be noticed that due to their high series equivalent resistance standard single-switch, single-ended converters (for instance boost and buck-boost topologies) cannot be used to implement the DRER converter. Since it demands very high duty-cycles to handle the voltage difference between a single PV module, Wind, Fuel cell and the 240V of the DC-bus. This high conversion ratio is achieved with a integration of Boost-Zeta DC-DC converter is proposed in this paper This DC-DC converter is based on the integration of the Boost and the Zeta converters. The DRER converter is comprised of a single-switch DC/DC converter with an input, middle section and output section [6-10][15-16]. Where the input section consists of PV source, Wind and Fuel cell. The switch and primary of the coupled-inductor composed of L_m , N_1 and N_2 . The middle section is given by secondary of the coupled-inductor and the capacitor C_z . Finally, the output section can be split into two parts. The output section of the Boost converter is comprised of a diode D_b and the capacitor C_{ob} , and the output section of Zeta converter is given by diode D_z , inductor L_o and the capacitor C_{oz} , where their connection is in stacked ($V_{ob}+V_{oz}$). Note that in the output section is the inductor L_o , therefore the output current has low ripple and the possibility of controlling this current. The converter is named Boost-Zeta integrated converter.

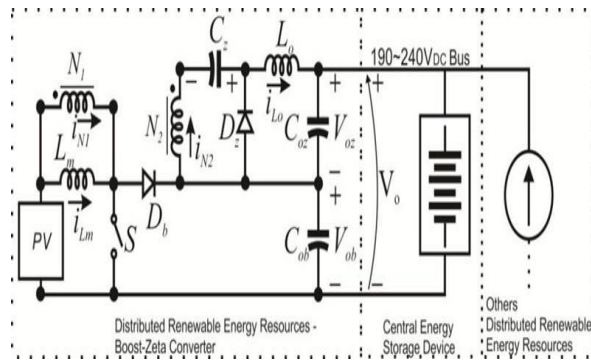


Fig. 1 Integrated Boost-Zeta converter

III. SYSTEM MODELING

The configuration of the microgrid proposed in this paper that is designed to operate either in the grid-connected or islanded mode. The main DG unit comprises a 40-kW PV array and a 15-kW PEMFC, which are connected in parallel to the dc side of the DG inverter 1 through dc/dc boost converters to regulate the dc-link voltage of the DG inverter at the desired level by delivering the necessary power. The PV array is implemented as the primary generation unit and the PEMFC is used to back up the intermittent generation of the PV array. When there is ample sunlight, the PV array operates in the MPPT mode to deliver maximum dc power PPV, which is discussed in detail, and the output voltage of the PV array is permitted to vary within an allowable range to ensure proper operation of the DG inverter. To maintain the level of the dc-link voltage VDC at the required level, the PEMFC supplements the generation of the PV array to deliver the necessary PFC. When the output voltage of the PV array falls below a preset limit, the PV array is disconnected from the DG unit and the PEMFC functions as the main generation unit to deliver the required power. A 30-Ah lithium-ion SB is connected to the dc side of DG inverter 2 through a bidirectional dc/dc buck-boost converter to facilitate the charging and discharging operations. During islanded operation, the role of the SB is to maintain the power balance in the micro grid which is given by

$$PDG + P_b = PL \tag{1}$$

where PDG is the power delivered by the main DG unit, is the SB power which is subjected to the charging and discharging constraints given by

$$P_b \leq P_{b,max} \tag{2}$$

and is the real power delivered to the loads. The energy constraints of the SB are determined based on the state-of-charge (SOC) limits which are given as

$$SOC_{min} < SOC < SOC_{max} \tag{3}$$

Although the SOC of the battery cannot be measured directly, it can be determined through several estimation methods presented. When the micro-grid operates is - landed from the distribution grid, the SB can operate in the charging, discharging, or idle mode depending on its SOC and PB. The EMS controls and monitors different aspects of power management, such as load forecasting, unit commitment, economic dispatch, and optimal power flow through a

centralized server. Important information, such as field measurements from smart meters, transformer tap positions, and circuit-breaker (CB) status are all sent to the centralized server for processing through Ethernet. During grid-connected operation, the distribution grid is connected to the microgrid at the point of common coupling (PCC) through a circuit breaker (CB). During off-peak periods when the cost of generation from the grid is low and if the SB's SOC is below the maximum SOC limit, the SB can be charged by the grid and the loads will be supplied by the main DG unit and the grid. During peak periods, when the cost of generation from the grid is high and if the SB's SOC is above the minimum SOC limit, the SB can deliver power to the grid to achieve peak shaving. When a fault occurs on the upstream network of the distribution grid, the CB operates to disconnect the microgrid from the distribution grid. The main DG unit and the SB are the sole power sources left to regulate the loads. In the case when the generation capacity of the main DG unit is unable to meet the total load demand, the SB is required to provide for the shortage in real and reactive power to maintain the power balance and stability of the microgrid.

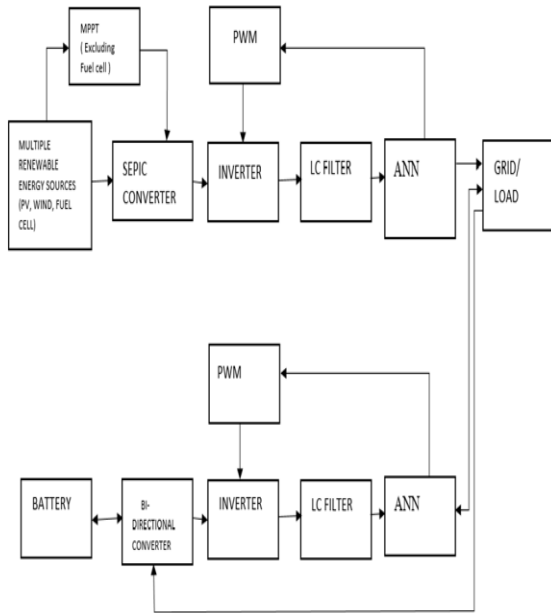


Fig. 2 Block Diagram of Proposed System

IV. DG INVERTER MODELING

The equivalent single-phase representation of the DG inverters for grid-connected and is-landed

operation. The switched voltage across the output of the j th DG inverter is represented by $U_j V_{dcj}$, where is the control input. The output of the DG inverter is interfaced with an LC filter represented by L_{fj} and C_{fj} to eliminate the high switching frequency harmonics generated by the DG inverter. The resistance models the loss of the DG inverter. The total load current i_L , which is the sum of the currents delivered to the load is given by

$$I_L = \sum_{k=1,2,3} I_{Lk} = i_{L1} + i_{L2} + i_{L3} \quad 4$$

and can be modeled as two components consisting of fundamental $i_{L,f}$ and $i_{L,h}$ harmonic with their peak amplitudes $i_{L,f}$ and $i_{L,h}$, respectively, and is represented i_L

$$\begin{aligned} i_L &= i_{L,f} + i_{L,h} = I_{L,f} \sin(\omega t - \phi_{L,f}) + \sum_{h=3,5,\dots}^N I_{L,h} \sin(h\omega t - \phi_{L,h}) \\ &= i_{L,f} \sin \omega t \cos \phi_{L,f} + i_{L,f} \cos \omega t \sin \phi_{L,f} + \sum_{h=3,5,\dots}^N I_{L,h} \sin(h\omega t - \phi_{L,h}) \\ &= i_{L,f,p} + i_{L,f,q} + i_{L,h} \end{aligned} \quad 5$$

where $\phi_{L,f}$ and $\phi_{L,h}$ are the respective phase angles of the fundamental and harmonic components of i_L , $i_{L,f,p}$ and $i_{L,f,q}$ and the instantaneous fundamental phase and quadrature components of i_L . To achieve unity power factor at the grid side, compensate for the harmonics in the load currents and concurrently achieve load sharing, the inverter of the DG unit supplies a current that is given by

$$i_{DGj} = (i_{L,f,p} - i_g) + i_{L,f,q} + i_{L,h} \quad 6$$

where i_g is the grid current. The distribution grid is supplied by a utility substation represented by a voltage source v_g during grid-connected operation, and is connected to the microgrid and the loads via a distribution line with resistance R_l and inductance L_l . In the grid-connected mode, the grid voltage is known and the microgrid shares the load demand with the grid. Hence to control the power delivered to the loads, the output current of the DG inverter is controlled using the current control mode (CCM).

During islanded operation, the microgrid will supply the overall load demand and it is required that the output voltage be regulated to a pure sine wave with a fixed magnitude. This can be achieved through the voltage-control mode (VCM).

To derive a state-space model for the DG inverter during both grid-connected and islanded operations, Kirchhoff's voltage and current laws are applied to the current loop and the following equations are obtained:

$$\frac{di_j}{dt} = -\frac{R_j}{L_{fj}} i_j - \frac{1}{L_{fj}} V_{DGj} + \frac{V_{dcj}}{L_{fj}} V_j \quad 7$$

$$\frac{dv_{DGj}}{dt} = \frac{1}{C_{fj}} i_j - \frac{1}{C_{fj}} i_{DGj} \quad 8$$

where i_j is the current passing through L_{fj} . Hence the grid connected DG inverter model can be written as

$$\dot{x}_{gj} = A_{gj}x_{gj} + B_{gj1}\dot{u}_j + B_{gj2}u_j \quad 9$$

$$y_{gj} = C_{gj}x_{gj} + D_{gj1}\dot{u}_j + D_{gj2}u_j \quad 10$$

where the subscripts g and j and represent the model of DG inverter during grid-connected operation.

$$A_{gj} = -\frac{R_j}{L_{fj}}; B_{gj1} = \left[-\frac{1}{L_{fj}} \ 0 \right]; C_{gj} = 1; \\ D_{gj1} = [0 \ -C_{fj}]; D_{gj2} = 0$$

x_{gj} is the state exogenous input, u_j is the control input and $y_{gj} = i_{DGj}$ is the output, which will be regulated to track the desired periodic reference waveform. During islanded operation, the frequency will change due to power imbalance in the microgrid. This change in frequency is detected by the EMS of the microgrid, which is used to manage and monitor the power dispatch by each DG unit. Based on the frequency change information, the EMS will require the main DG unit and the SB to generate the necessary power to meet the overall load demand in the microgrid. During islanded operation, DG inverter can be modeled as

$$\dot{x}_{ij} = A_{ij}x_{ij} + B_{ij1}\dot{u}_j + B_{ij2}u_j \quad 11$$

where the subscript denotes the model of the DG inverter during islanded operation and

$$A_{ij} = \begin{bmatrix} -\frac{R_i}{L_{fj}} & -\frac{1}{L_{fj}} \\ \frac{1}{C_f'} & 0 \end{bmatrix}; \\ B_{ij1} = \begin{bmatrix} 0 \\ -\frac{1}{C_f'} \end{bmatrix}; B_{ij2} = \begin{bmatrix} \frac{V_{dcj}}{L_{fj}} \\ 0 \end{bmatrix}; \\ C_{ij} = \begin{bmatrix} 0 & 1 \\ 1 - \frac{C_{fj}}{C_f'} & 0 \end{bmatrix}; D_{ij1} = \begin{bmatrix} 0 \\ \frac{C_{fj}}{C_f'} \end{bmatrix}; \\ D_{ij2} = \begin{bmatrix} 0 \\ 0 \end{bmatrix}$$

$$C_f' = \sum_{j=1}^2 C_{fj}; x_{ij} = [i_j V_{DGj}]^T \text{ is the state vector.}$$

V. CONTROL DESIGN

This paper proposes a novel MPC algorithm for the control of the DG inverters of the microgrid. The

proposed algorithm is a newly developed MPC algorithm specifically designed for fast-sampling systems, to track periodic signals so as to deal with the dual-mode operation of the microgrid. The algorithm decomposes the MPC optimization into a steady-state sub-problem and a transient sub-problem, which can be solved in parallel in a receding horizon fashion. Furthermore, the steady-state sub problem adopts a dynamic policy approach in which the computational complexity is adjustable. The decomposition also allows the steady-state sub-problem to be solved at a lower rate than the transient sub-problem if necessary. These features help to achieve a lower computational complexity and make it suitable for implementation in a fast-sampling system like our microgrid applications. In the simulation studies in this paper, the sampling interval is chosen as 0.2ms, which is considered pretty small in conventional MPC applications, but necessary for the high order of harmonics being tackled for our problem.

Sampling in the range of tens of kHz is possible with state-of-the-art code generation techniques. It is noted that in either the grid-connected or the islanded operation, the state-space model after time-discretization will take the form

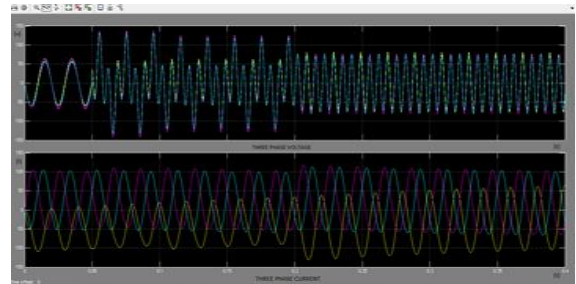
$$x^+ = Ax + B_1\omega + B_2u \quad 12$$

$$y = Cx + D_1\omega + D_2u \quad 13$$

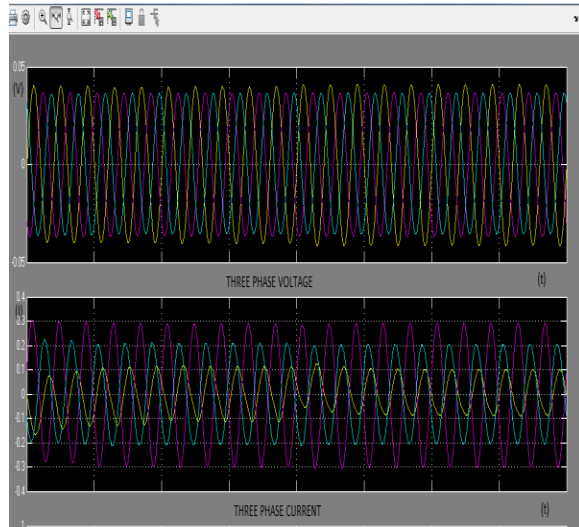
where the superscript $+$ represents the time-shift operator (with sampling interval), and the exogenous signal ω is periodic.

VI. CONCLUSION

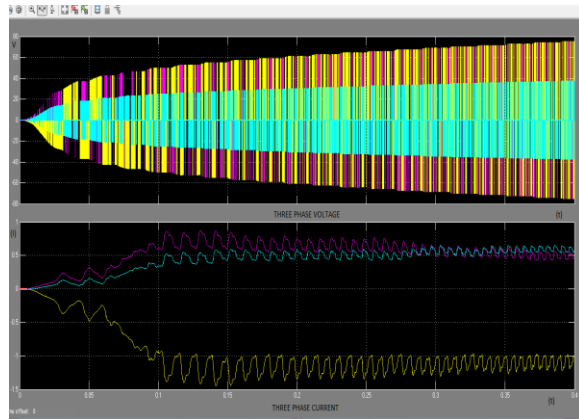
This paper concludes that energy is harvested from multiple energy resources and its is supplied to both grid/load side and to the battery. When insufficient energy occurs at grid side, battery supplies energy to the load. ANN controller is used to maintain the constant output voltage at the load side.



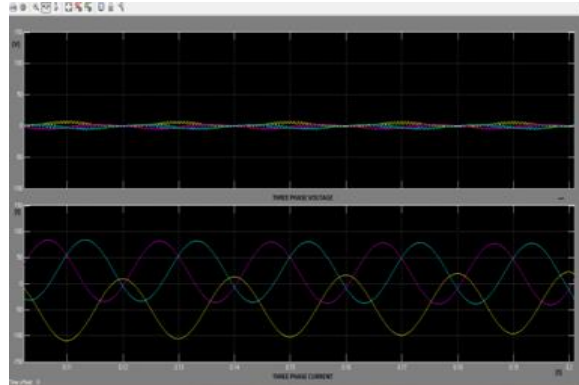
PV Output



Wind Output



Fuel Cell Output



Battery output

REFERENCES

[1] M. Lai; C. T. Pan; M. C. Cheng, "High-Efficiency Modular High Step-Up Interleaved Boost Converter for DC-Microgrid

Applications," *IEEE Trans. Ind. Appl.*, vol.48, no.1, pp.161-171, Jan.-Feb. 2012.

[2] P. Xuwei. A. K. Rathore, U. R. Prasanna, "Novel Soft-Switching Snubberless Naturally Clamped Current-Fed Full-Bridge Front-End-Converter-Based Bidirectional Inverter for Renewables, Microgrid, and UPS Applications," *IEEE Trans. Ind. Appl.*, vol.50, no.6, pp.4132-4141, Nov.-Dec. 2014.

[3] M. Farhadi, O. A. Mohammed, "Real-Time Operation and Harmonic Analysis of Isolated and Non-Isolated Hybrid DC Microgrid," *IEEE Trans. Ind. Appl.*, vol.50, no.4, pp.2900-2909, July-Aug. 2014.

[4] M. Farhadi, O. A. Mohammed, "Performance Enhancement of Actively Controlled Hybrid DC Microgrid Incorporating Pulsed Load," *IEEE Trans. Ind. Appl.*, vol.51, no.5, pp.3570-3578, Sept.-Oct. 2015.

[5] R. Ahmadi, M. Ferdowsi, "Improving the Performance of a Line Regulating Converter in a Converter-Dominated DC Microgrid System," *IEEE Trans. in Smart Grid*, vol.5, no.5, pp.2553-2563, Sept. 2014.

[6] Z. Liang; R. Guo; J. Li; A. Q. Huang, "A High-Efficiency PV Module-Integrated DC/DC Converter for PV Energy Harvest in FREEDM Systems," *IEEE Trans Power Elect.*, vol.26, no.3, pp.897-909, March 2011.

[7] A. Q. Huang, M. L. Crow, G. T. Heydt, J. P. Zheng, S. J. Dale, "The Future Renewable Electric Energy Delivery and Management (FREEDM) System: The Energy Internet," *Proceedings of the IEEE*, vol.99, no.1, pp.133-148, Jan. 2011.

[8] F. Xue, Y. Zhao, R. Yu, W. Yu; A. Q. Huang, "Stationary energy storage system based on modular high voltage battery modules," *IEEE First International Conference DC Microgrids (ICDCM)*, 7-10 June 2015.

[9] A. Q. Huang, "Renewable energy system research and education at the NSF FREEDM systems center," *IEEE Power & Energy Society General Meeting*, pp.1-6, 26-30 July 2009.

[10] A. Q. Huang, "FREEDM system - a vision for the future grid," *IEEE inPower and Energy Society General Meeting*, pp.1-4, 25-29 July 2010.

- [11] O. Khan, W. Xiao; H. H. Zeineldin, "Gallium-Nitride-Based Submodule Integrated Converters for High-Efficiency Distributed Maximum Power Point Tracking PV Applications," *IEEE Trans. Ind.Elect.*, vol.63, no.2, pp.966-975, Feb. 2016.
- [12] D. Bol, E. H. Boufouss, D. Flandre, J. De Vos, "A 0.48mm² 5 μ W-10mW indoor/outdoor PV energy-harvesting management unit in a 65nm SoC based on a single bidirectional multi-gain/multi-mode switched-cap converter with supercap storage," in *European Solid-StateCircuits Conference (ESSCIRC)*, pp.241-244, 14-18 Sept. 2015.
- [13] I. Laird, D. D. C. Lu, "High Step-Up DC/DC Topology and MPPT Algorithm for Use with a Thermoelectric Generator," *IEEE Trans. onPower Elect.*, vol.28, no.7, pp.3147-3157, Jul. 2013.
- [14] N. Katayama, S. Tosaka, T. Yamanaka, M. Hayase, K. Dowaki, S. Kogoshi, "New Topology for DC-DC Converters Used in Fuel Cell-Electric Double Layer Capacitor Hybrid Power Source Systems for Mobile Devices," *IEEE Trans. Ind. Appl.*, vol.52, no.1, pp.313-321, Jan.-Feb. 2016.
- [15] K. E. Holbert, L. L. Grable, A. Overbay, B. J. O. Nzekwe, "FREEDM Precollege Programs: Inspiring Generation Y to Pursue Careers in the Electric Power Industry," *IEEE Trans. Power Syst.*, vol. 29, n. 4, pp. 1888-1896, 2014.
- [16] P. Tatcho, H.Li, Y.Jiang, L.Qi, "A Novel Hierarchical Section Protection Based on the Solid State Transformer for the Future Renewable Electric Energy Delivery and Management (FREEDM) System," *IEEE Trans. Smart Grid*, vol. 4, n. 2, pp. 1096-1105, 2013.